

Invited paper

EXPERIMENTAL INVESTIGATION OF AN ANNULAR DIFFUSER FOR AXIAL FANS AT DIFFERENT INFLOW PROFILES

by

**Johannes WALTER^{a*}, Dieter WURZ^b, Stefan HARTIG^b,
and Martin GABI^a**

^aInstitute of Fluid Machinery, Karlsruhe Institute of Technology, Karlsruhe, Germany

^bESG, Emission Measurement Technology and Fluid Mechanics, Baden-Baden, Germany

Original scientific invited paper
<https://doi.org/10.2298/TSCI160408183W>

Axial fans are used in power plants for fresh air supply and flue gas transport. A typical configuration consists of an axial fan and annular diffuser which connects the fan to the following piping. In order to achieve a high efficiency of the configuration, not only the components have to be optimized but also their interaction. The present study focuses on the diffuser of the configuration. Experiments are performed on a diffuser-piping configuration to investigate the influence of the velocity profile at the fan outlet on the pressure recovery of the configuration. Two different diffuser inlet profiles are generated, an undisturbed profile and a profile with the typical outlet characteristics of a fan. The latter is generated by the superposition of screens in the inlet zone. The tests are conducted at a high Reynolds number ($Re \approx 4 \cdot 10^5$). Mean velocity profiles and wall shear stresses are measured with hydraulic methods (Prandtl and Preston tubes). The results show that there is a lack of momentum at the outer wall of the diffuser and high shear stresses at the inner wall in case of the undisturbed inflow profile. For the typical fan outlet profile it is vice versa. There are high wall shear stresses at the outer wall while the boundary layer of the inner wall lacks momentum. The pressure recovery of the undisturbed inflow configuration is in good agreement with other studies.

Key words: *annular diffuser, flow separation, fan outflow profile, Preston method, pressure recovery*

Introduction

A large part of the total pressure increase of a fan is often available as dynamic pressure at the outlet. Annular diffusers are used to reduce the dynamic pressure downstream the impeller of the axial fan. Figure 1 shows a common fan-diffuser configuration in a thermal power plant for fresh air supply. In order to achieve a high efficiency of the configuration, the dynamic pressure needs to be converted into a static pressure increase. The outflow profile of the fan respectively the diffuser inflow profile depends on the operation point of the fan and

* Corresponding author, e-mail: walter@kit.edu

can therefore affect the diffuser efficiency. The goal of this study is to determine the pressure recovery coefficient cp of the configuration for different inflow profiles.

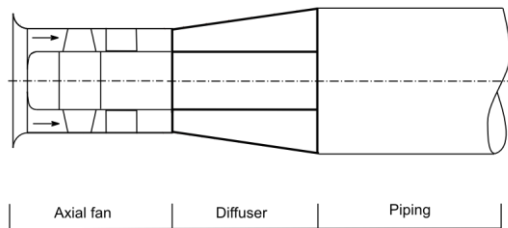


Figure 1. State-of-art fan-diffuser configuration

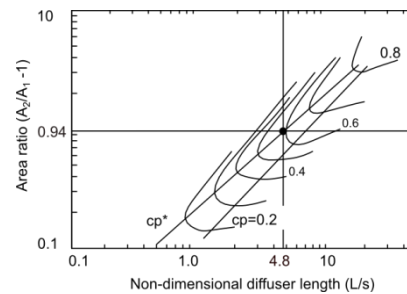


Figure 2. Diffuser performance chart [1]

Annular diffusers are investigated in several studies. The most notable work was conducted by Sovran and Klomp [1]. They investigated pressure recovery for different diffuser lengths and area ratios for inflow profiles with low aerodynamic blockage B . Their diffuser performance chart is commonly used as a guideline for diffuser construction. Stevens and Williams [2] examined the performance of two annular diffuser configurations. They performed experiments for an undisturbed inlet profile, a fully developed profile and one with increased turbulent mixing. According to their research the inlet profile and the turbulence intensity have a strong impact on the overall pressure recovery. In 1982, Dierksen published datasets of velocity profiles in annular diffusers measured by Laser Doppler Velocimetry [3]. Japikse published a study on the influence of geometry, swirl and blockage on the annular diffuser flow [4]. He derived a correlation based on measurements to estimate the diffuser performance.

It is necessary to understanding the effect of the fan outflow profile on the diffuser flow to improve the performance of fan-diffuser-piping configurations. In the present study, a fan outflow profile is reproduced and the diffuser flow characteristics are analysed. The results are compared to the flow characteristics of the diffuser with undisturbed inflow. In order to achieve realistic reference data at the diffuser inlet, in-situ profile measurements at the outlet of an axial fan in a coal-fired power plant are used as reference. Besides the velocity profiles and the pressure recovery a closer look is taken on the wall shear stress distribution in the diffuser and downstream to characterize the flow stability. Therefore a test rig is constructed. The annular diffuser is designed according to state of art diffusers in power plants at a laboratory scale. The geometry of the diffuser is chosen according to the guideline of Sovran and Klomp, fig. 2. By means of their chart the pressure recovery cp for a given diffuser length (cp^*) can be determined. A pressure recovery cp of 0.59 is expected for the investigated diffuser.

Experimental apparatus and methods

The test rig is shown in fig. 3. A filter is installed in front of the inlet nozzle to homogenize the inflow and keep the airflow clean. The entry section ensures the laminar to turbulent transition of the boundary layer. The test rig is designed to conduct experiments for different inflow profiles. Therefore an installation section for screens is arranged 1.5s

The fan outflow profile is reconstructed at the inlet of the test rig diffuser by the superposition of two screens, fig. 5. The screens are mounted in the installation section upstream the annular diffuser of the rig.

According to Traupel [5] a Reynolds independence of the diffuser flow is achieved at Reynolds Numbers $Re > 1 \cdot 10^5$ and Mach Numbers $Ma < 0.7$. In the present study experiments are performed at $Re \approx 4 \cdot 10^5$ and $Ma \approx 0.1$.

Measurement technique

The velocity profiles are measured with a Prandtl probe and a MKS Baratron pressure converter. An integration time of 10 seconds is used for averaging. The boundary layer displacement correction according to Mc-Millan is applied. This correction can be found in [6]. The wall shear stress is determined with an extended Preston method CPM3 [7]. This method is based on the extended law of the wall according to Szablewski (eq. 1), which considers an adverse pressure gradient:

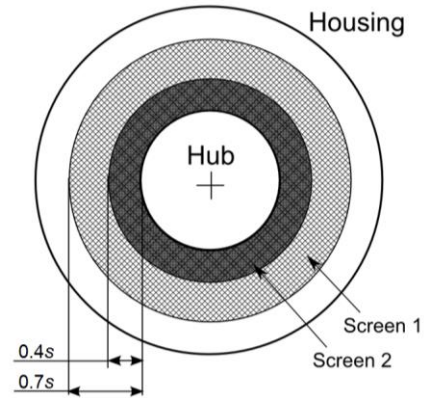


Figure 5. Screens for inflow disturbance

$$u^+ = \int_0^{y^+} \frac{2(1 + p^+ y^+)}{1 + \sqrt{1 + 4(\kappa y^+)^2 (1 + p^+ y^+) \left[1 - \exp\left(\frac{y^+}{A^+} \sqrt{1 + p^+ y^+}\right)\right]^2}} dy^+ \quad (1)$$

$$u^+ = \frac{c}{u_\tau}, \quad y^+ = \frac{cy}{\nu}, \quad p^+ = \frac{\nu}{\rho u_\tau^3} \frac{dp}{dx} \quad (2)$$

The parameters κ , A^+ , p^+ have to be determined to find the local law of the wall. Near wall velocity measurements are conducted with pressure probes. The law of the wall (1) is transferred in its dimensional formulation using the friction velocity u_τ . A parameter variation of u_τ , κ , A^+ , p^+ is done until an appropriate fit of the measured near wall profile and law of the wall is found. The interested reader is referred to Nitsche *A computational Preston tube method* [7] for more detailed information. The turbulence intensity Tu is measured at the diffuser inlet. Therefore a 1-D single wire probe with a Dantec Streamline hot wire system is used.

Measurement sections

Velocity measurements are conducted at the diffuser inlet (MP1), the diffuser outlet (MP4) and downstream the diffuser (MP5, MP6, MP7) in four axes (0° , 90° , 180° , 270°), fig. 6. At MP2 and MP3 one axis (0°) is measured. The turbulence intensity Tu is recorded at diffuser inlet (MP1, 0°). The wall shear stresses τ_{wall} and the near wall velocity profiles are measured at one circumferential position (0°).

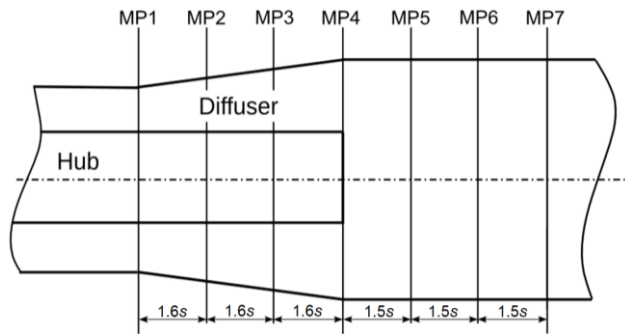


Figure 6. Measurement sections

Results and discussion

The inlet conditions in the diffuser are described in tab. 1. The mean turbulence intensity (Tu) at the inlet of the undisturbed inflow configuration is $Tu = 5.4\%$ and in the disturbed configuration $Tu = 5.7\%$. In both configurations, a Reynolds independency is expected ($Re > 1 \cdot 10^5$). In order to quantify the blockage of the profile at the inlet, the aerodynamic blockage B (eq. 3) is introduced analogous to [1, 4]:

$$B = 1 - \frac{1}{A} \int \frac{c_{ax}}{c_{ax,max}} dA \quad (3)$$

Table 1. Inflow conditions to the diffuser

Configuration	$c_{ax,inlet}$ [m/s]	$Re_{hyd,inlet}$ [-]	Tu_{inlet} [%]	B
Undisturbed profile	24.2	$3.9 \cdot 10^5$	5.4	0.055
Disturbed profile	24.8	$4.0 \cdot 10^5$	5.7	0.17

Flow in the annular diffuser

Figure 7 shows the development of the velocity profile in the diffuser. The strong dependence of the diffuser outflow profile on the inflow characteristic is clearly visible. The undisturbed profile develops a velocity maximum close to the hub. The velocity maximum of the disturbed inlet profile is located in the outer region of the annular gap. This maximum gets amplified in the diffuser. Flow separation is detected at the hub of the diffuser outlet. In order to quantify the flow homogeneity the distortion parameter D (eq. 4) is introduced [8]. If the parameter D equals zero, the flow profile is uniform.

$$D = \left[\frac{A}{\dot{V}^2} \int_{r_i}^{r_o} c_{ax}^2 dA \right] - 1 \quad (4)$$

The distortion D grows strongly monotonous in the diffuser for the undisturbed inflow, fig. 8. The level of $D = 0.1$ is reached at the diffuser outlet. The disturbed inflow starts at $D = 0.03$ and reaches its maximum at $x/L = 2/3$ with $D = 0.15$. Further downstream the distortion decreases slightly ($D = 0.14$ at diffuser outlet).

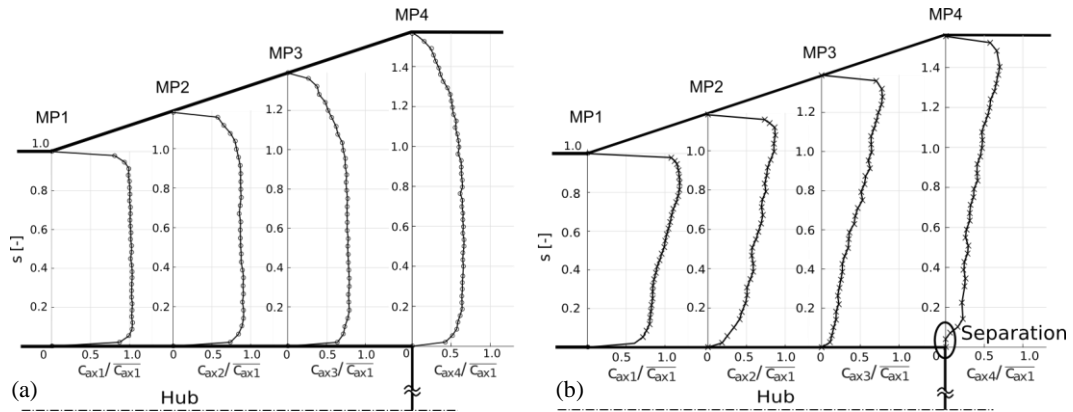


Figure 7. Velocity profiles in the annular diffuser; (a) undisturbed inflow and (b) disturbed inflow

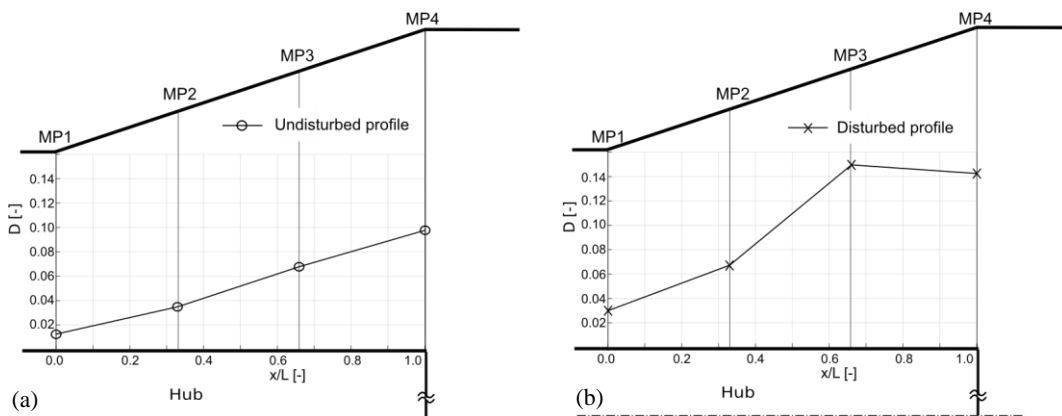


Figure 8. Profile distortion of the flow; (a) undisturbed inflow and (b) disturbed inflow

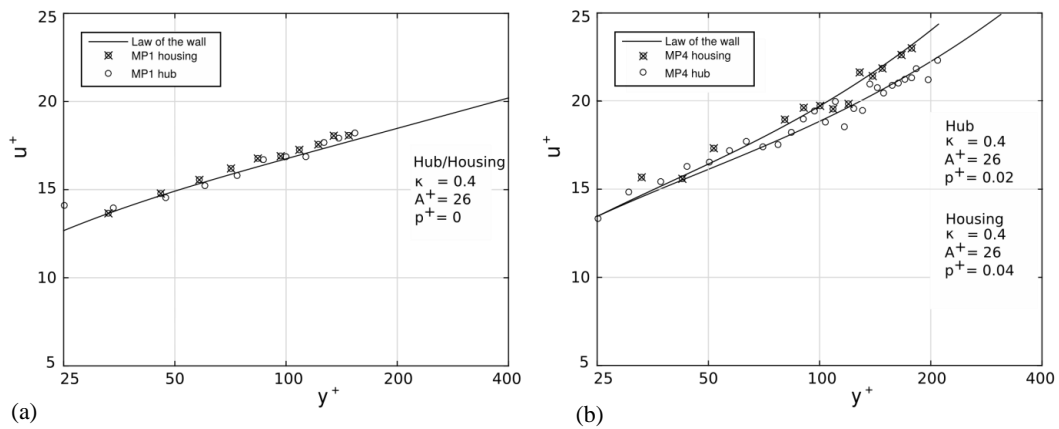


Figure 9. Near wall velocity profiles for undisturbed inflow; (a) diffuser inlet and (b) diffuser outlet

In order to take a closer look on the flow stability in the annular diffuser, the wall shear stress is analysed at the hub and the housing of the diffuser. Therefore the CPM3 Method is used. The CPM3 leads to the law of the wall and the corresponding wall shear stress. In figs. 9 and 10, the law of the wall and the near wall velocity measurements are plotted. There is a good agreement of measurement points and the law of the wall.

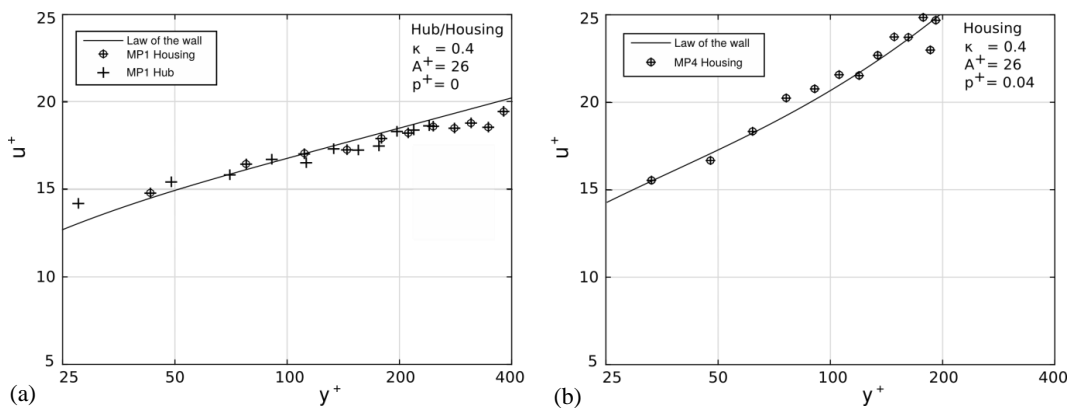


Figure 10. Near wall velocity profiles for disturbed inflow; (a) diffuser inlet and (b) diffuser outlet

Both inflow profiles follow the law of the wall for $\kappa = 0.4$ and $A^+ = 26$ in the near wall region at the inlet (MP1) figs. 9 and 10, left). The pressure increase in the diffuser has to be considered at the outlet (MP4). The best fit for the extended law of the wall is found for $p^+ = 0.02$ at the hub and for $p^+ = 0.04$ at the housing (undisturbed inflow profile, fig. 9 right). The law of the disturbed profile is approximated with $p^+ = 0.04$ at the housing in MP4 (fig. 10 right). The wall shear stress at the hub cannot be determined due to flow separation.

Next, the flow stability is discussed. There are different parameters indicating a stable forward flow. An overview is given in [9]. In this study a simple approach is chosen. It is assumed that the wall shear stress of a flat plate at corresponding outer flow velocity and distance indicates a stable forward flow. The wall shear stress of the diffuser flow is related to the theoretical wall shear stress of a flat plate.

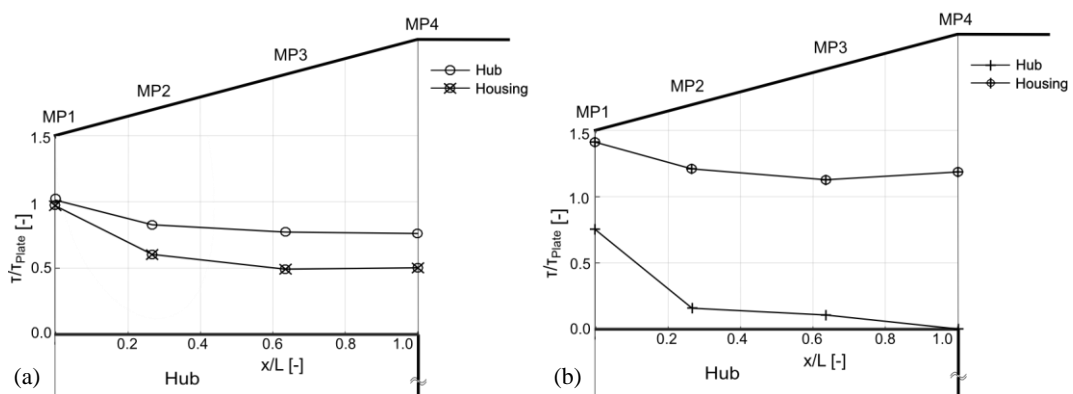


Figure 11. Wall shear stress distribution in the annular diffuser; (a) undisturbed inflow and (b) disturbed inflow

In this study a formulation according to Schlichting [10] is used to calculate the wall shear stress along a plate:

$$\tau_{Wall} = \frac{1}{2} \rho c_f c_\infty^2, \quad \text{where } c_f = [2 \log_{10}(\text{Re}_x) - 0.65]^{-2.3} \quad (5)$$

Figure 11 shows the wall shear stress distribution along the hub and the housing for both inflow profiles. The wall shear stress at the inlet of the undisturbed inflow configuration is close to the wall shear stress of a flat plate. It decreases in the diffuser. At the outlet it is only 76 % (hub) respectively 51% (housing) of the corresponding wall shear stress of a flat plate (fig. 11 left).

Next the disturbed inflow is discussed (fig. 11 right). The wall shear stress at the housing of the diffuser inlet is 1.4 times higher than the corresponding stress of a flat plate. In the diffuser this maximum value decreases to a local minimum of 1.12 at 2/3 of the diffuser length and rises again to 1.19 at the diffuser outlet.

The wall shear stress at the hub at the inlet is only 75% of the reference value and it decreases in mean flow direction. The flow separates close to the diffuser outlet.

Flow downstream the annular diffuser

The flow downstream the annular diffuser is investigated. The hub ends at the outlet of the annular diffuser. This sudden increase of area causes a wake area downstream the hub. Figure 12 shows the flow profiles downstream the diffuser. The wake area is filled for both configurations at $x/s = 3$ (MP6). They reach a similar level of homogeneity $D \approx 0.8$ at $x/s = 1.5$ (MP5), fig. 13.

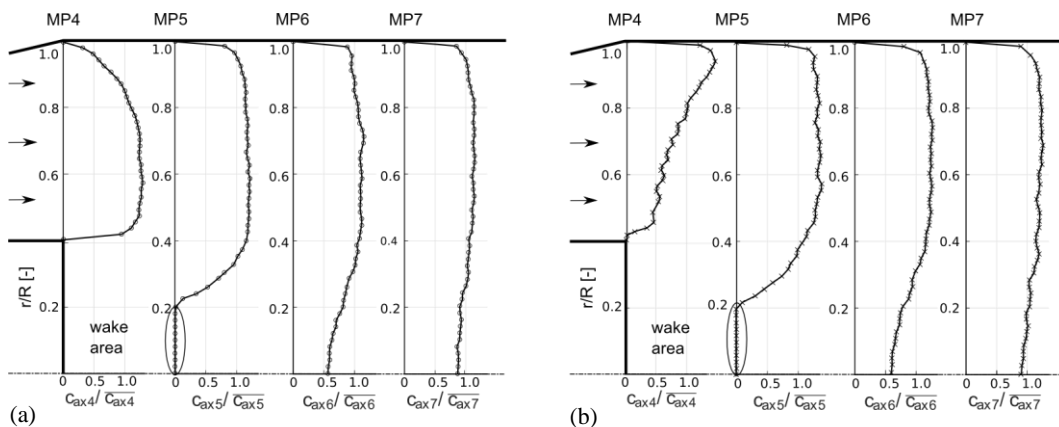


Figure 12. Velocity profile downstream the hub; (a) undisturbed inflow and (b) disturbed inflow

The near wall velocity profiles and the law of the wall are plotted at different axial positions. The parameters of the law of the wall are $\kappa = 0.42$ and $A^+ = 26$. The best agreement is reached at MP7 where the effect of the wake area of the hub is nearly vanished, fig. 14.

Downstream the hub the wall shear stress at the housing rises. The maximum of the wall shear stress is reached at MP6 for the undisturbed inflow and at MP5 for the disturbed inflow. Further downstream the wall shear stress decreases again, fig. 15.

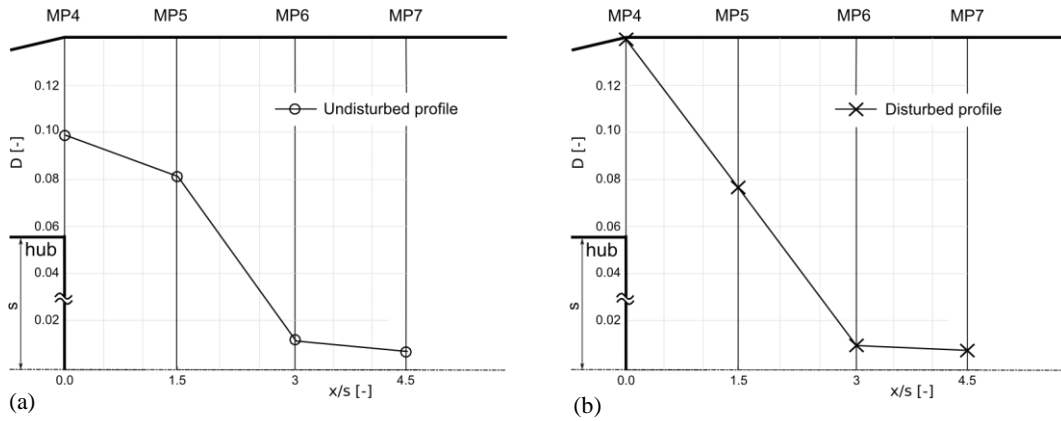


Figure 13. Flow distortion downstream the hub; (a) undisturbed inflow and (b) disturbed inflow

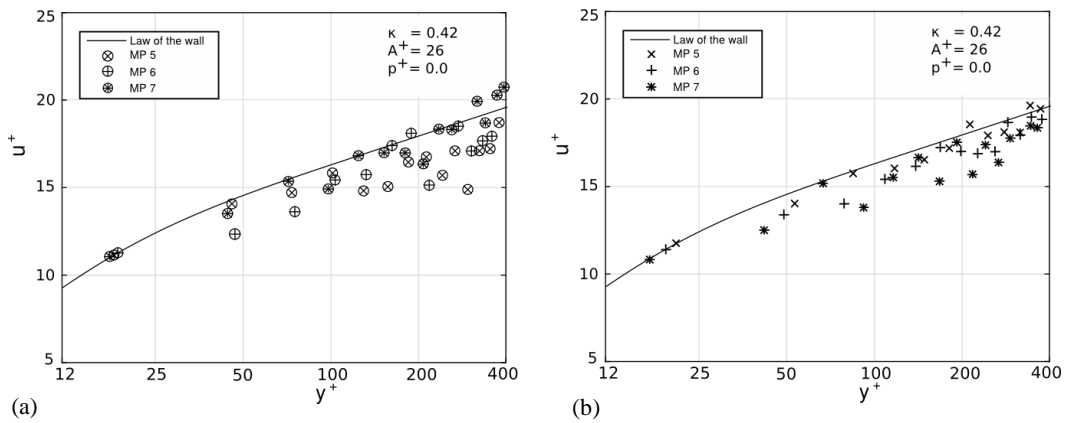


Figure 14. Near wall velocity profiles downstream the hub; (a) undisturbed inflow and (b) disturbed inflow

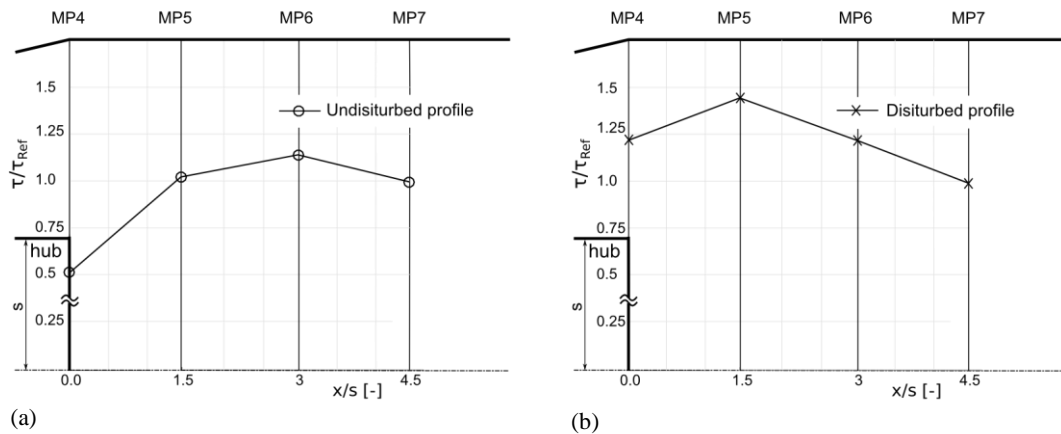


Figure 15. Wall shear stress downstream the hub at the housing of the cylindrical pipe; (a) undisturbed inflow and (b) disturbed inflow

Pressure recovery of the configuration

The configuration can be split in two kinds of diffusers, an annular diffuser and a Carnot diffuser (end of hub). The maximum pressure coefficient for an inviscid flow can be calculated as follows:

$$cp_{ideal} = \frac{P_{s,i} - P_{s,1}}{P_{dyn,1}} = 1 - \frac{1}{AR^2} \quad (6)$$

In order to get a more realistic estimation of the pressure recovery, the recovery mechanisms of this configuration are separately analysed. The recovery coefficient cp is divided into three components:

$$cp = cp_1 + cp_2 + cp_{profile} \quad (7)$$

where cp_1 is pressure recovery of the annular diffuser, cp_2 is pressure recovery of the Carnot diffuser and $cp_{profile}$ is pressure recovery due to rehomogenisation of the velocity profile downstream the hub.

There are various studies on pressure recovery cp_1 in annular diffusers [1, 2, 4]. The design chart of Sovran and Klomp [1] leads to the pressure recovery coefficient. However, the influence of a distorted inflow profile is not considered. A more realistic estimation is given by Japikse [5]. His correlation takes additionally the influence of the area ratio (AR) and the inlet blockage (B) into account:

$$cp = cp_{ideal} \eta(AR) \eta(B) \quad (8)$$

The pressure recovery cp_2 of the dump diffuser is calculated according to Carnot formula:

$$cp_2 = \frac{P_5 - P_4}{\frac{\rho}{2} c_{1,ax}^2} = 2 \frac{A_1^2}{A_4 A_5} \left(1 - \frac{A_4}{A_5} \right) \quad (9)$$

The outflow profile of the annular diffuser is inhomogeneous. The flow profile homogenizes again downstream the hub, figs. 12 and 13. This effect causes a static pressure rise, which can be calculated by the following formula:

$$cp_{profile} = \left(\frac{A_1}{A_4} \right)^2 D_4 - \left(\frac{A_1}{A_i} \right)^2 D_i \quad (10)$$

The experimentally determined pressure recovery coefficient cp at measurement plane 4 (diffuser outlet) is 0.54 for the undisturbed inflow and 0.43 for the disturbed inflow, fig. 16. This result reflects the influence of the increased inlet blockage B of the configuration with disturbed inflow. Japikse's correlation for annular diffuser performance leads to results which are close to the experiments ($cp_{MP4, disturbed Profile} = 0.52$, $cp_{MP4, undisturbed Profile} = 0.44$). Downstream the annular diffuser two pressure recovery mechanisms are combined, the pressure recovery of the Carnot diffuser cp_2 and the pressure recovery due to the rehomogenisation of the profile $cp_{profile}$. The pressure recovery of the Carnot diffuser is dependent on the geometry (for this configuration $cp_2 = 0.072$ according to Carnot). The reduction of the profile distortion leads to a static pressure recovery $cp_{Profile, disturbed inflow} = 0.031$ respectively $cp_{Profile, undisturbed inflow} = 0.021$ at MP7. In total, the pressure recovery of the undisturbed configuration $cp_{undisturbed inflow}$ is 0.61 and for the disturbed inflow $cp_{disturbed inflow} = 0.54$ according to the correlations. These results are in good agreement with the measurement

of the static pressure rise in the configuration $cp_{exp,undisturbed\ inflow} = 0.60$ and $cp_{exp,disturbed\ inflow} = 0.55$.

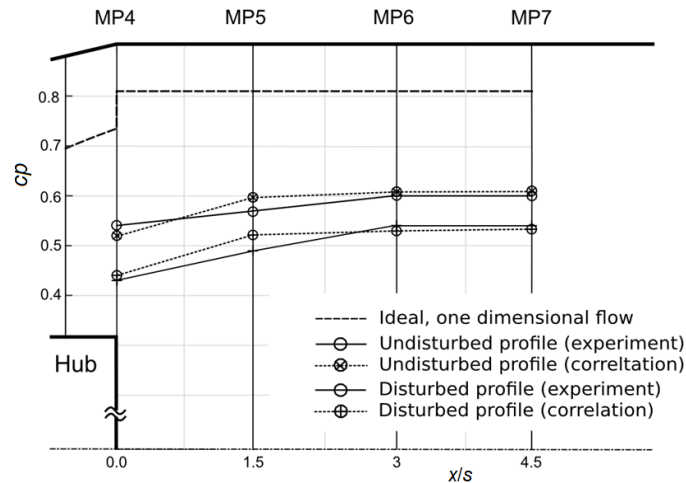


Figure 16. Static pressure recovery of the configuration (experiment and correlation)

Conclusions

The flow characteristic in the diffuser strongly depends on the inlet profile. While the undisturbed profile leads to a stable forward flow at the hub, the typical fan outflow profile (disturbed profile) shows low wall shear stresses at the hub and thus has the tendency to separate there. The pressure recovery of the annular diffuser is also influenced by the inflow profile. The correlation of Japikse could be confirmed by the measurements. Downstream the annular diffuser a further pressure rise is caused by the sudden enlargement of the area (Carnot diffuser) and the rehomogenization of the velocity profile in the cylindrical pipe. The wake area downstream the hub is filled up and the velocity peaks are attenuated. The pressure recovery for the configuration with undisturbed inflow is 60% in MP7. The disturbed inflow configuration disturbed inflow converts 55% of dynamic pressure into static pressure (MP7).

Nomenclature

A – cross section, [m²]
 A^+ – damping parameter, [-]
 a – speed of sound in air, [ms⁻¹]
 AR – area ratio, [-]
 B – aerodynamic blockage, [-]
 c – flow velocity, [ms⁻¹]
 cp – pressure recovery, [-]
 D – flow distortion parameter, [-]
 D_H – hydraulic diameter, [m]
 L – diffuser length, [m]
 Ma – Mach number ($= v/a$), [-]
 Pr_t – turbulent Prandtl number, [-]
 p – pressure, [Pa]
 Δp_{rel} – relative pressure difference, [-]
 p^+ – nondimensional pressure increase, [-]

p – dynamic pressure, [Pa]
 p_s – static pressure, [Pa]
 R – radius of the cylindrical pipe, [m]
 r – radial coordinate, [m]
 r_H – radius of the hub, [m]
 Re – Reynolds number ($= D_H \cdot c/\nu$), [-]
 s – annular gap height at diffuser inlet, [m]
 s_i – annular gap position ($= r - r_H$), [-]
 Tu – turbulence intensity, [%]
 u_r – friction velocity, [ms⁻¹]
 x – coordinate [m]

Greek symbols

κ – Von Karman constant, [-]
 ν – kinematic viscosity, [m²s⁻¹]

References

- [1] Sovran, G., Klomp, E. D., Experimentally Determined Optimum Geometries for Rectilinear Diffusers with Rectangular, Conical or Annular Cross-Section, *Fluid Mechanics of Internal Flow* (Ed. Gino Sovran), Warren, Mich., USA, 1967, pp. 270-319
- [2] Stevens, S. J., Williams, G. J., The Influence of Inlet Conditions on the Performance of Annular Diffusers, *J. of Fluids Eng.*, 102 (1980), 3, pp. 357-363
- [3] Dierksen, J. M., A Study of Annular Diffuser Flow Using A Photon-Correlating Laser Doppler Anemometer, M. Sc. Thesis, Airforce Inst of Tech Wright-Patterson AFB OH School of Engineering, 1983
- [4] Traupel, W., *Thermische Turbomaschinen: Erster Band Thermodynamisch-stroemungstechnische Berechnung (Thermal Turbomachinery: First Edition Thermodynamic and Aerodynamic Design – in German)*, Springer-Verlag, Berlin, 2013
- [5] Japikse, D., Correlation of Annular Diffuser Performance with Geometry, Swirl, and Blockage, *Proceedings, 11th NASA/OSU Thermal and Fluids Analysis Workshop, 10th World Energy Conference*, Cleveland, O., USA, 2002, pp. 107-118
- [6] Walter, W., *Stroemungsmesstechnik: Lehrbuch fuer Aerodynamiker, Stroemungsmaschinenbauer Lueftungs-und Verfahrenstechniker ab 5. Semester (Flow Measurement Technology: Course Book for Engineers from the 5th Semester – in German)*, Springer-Verlag, Berlin, 2013
- [7] Nitsche, W., *et al.*, A Computational Preston Tube Method, *Turbulent Shear Flows*, 4 (1985), 3, pp. 261-276
- [8] Cherry, E. M., *et al.*, Three-Dimensional Velocity Measurements in Annular Diffuser Segments Including the Effects of Upstream Strut Wakes, *Int. J. of Heat and Fluid Flow*, 31 (2010), 4, pp. 569-575
- [9] Cebeci, T., *et al.*, Calculation of Separation Points in Incompressible Turbulent Flows, *J. of Aircraft*, 9 (2010), 9, pp. 618-624
- [10] Schlichting, H., *Boundary Layer Theory*, Springer-Verlag, Berlin, 1987